

The Common Inlet Configuration: An Advanced Boundary Layer Ingestion Engine Integration Concept

Michaël Méheut^{*†}, Olivier Atinault^{*} and Sébastien Defoort[§]

^{*}ONERA, Université Paris-Saclay, Meudon, France

[§]ONERA, Université de Toulouse, Toulouse, France

michael.meheut@onera.fr, olivier.atinault@onera.fr, sebastien.defoort@onera.fr

[†] Corresponding Author

Abstract

This paper details design activities performed at ONERA on the Common Inlet Concept. This configuration features two turbofans fed by a common circular inlet around the fuselage, split in two parts, one half for each engine. The purpose of that kind of inlet is to ingest the whole boundary layer around the fuselage, in order to maximise the performance benefit of such an extreme BLI concept. A detailed aerodynamic design of the concept is proposed together with a far-field exergy based analysis to assess its aero-propulsive performance. On top of this, a comprehensive performance analysis of the configuration based on advanced OAD models is provided for two missions (business jet and SMR) to evaluate the benefits of the Common Inlet at aircraft level.

1. Introduction

Boundary Layer Ingestion is one of the most promising concepts that would help improving aircraft aero-propulsive performance. Many studies ([1] to [12]) have already highlighted the benefit of that technology, either at Conceptual using low fidelity models ([1], [5], [9], [10]) or using high-fidelity CFD (Computational Fluid Dynamics) simulations ([2], [3], [7], [8], [11], [12]). In the scope of the European Clean Sky 2 (ITD Airframe), ONERA and DLR investigated several unconventional engine integration solutions that could significantly reduce the environmental impact of air transportation in a near future. A stepwise analysis process was applied in order to cover a wide design space on the one hand, and to allow for deep analyses of the most promising concepts on the other. A downselection process in three steps was defined and applied to two different aircraft missions:

- Small Medium Range (SMR) mission based on CeRAS Top Level Aircraft Requirements (TLARs) [13];
- Low Speed Business Jet (LSBJ) mission (transonic cruise conditions).

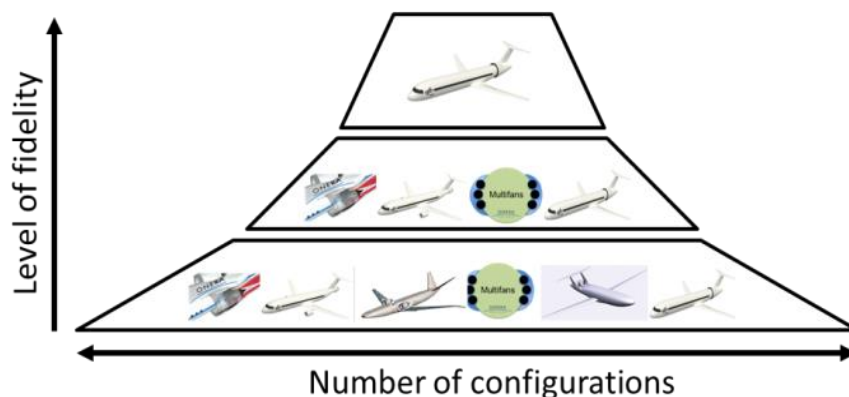


Figure 1 - Overview of the evaluation process.

This paper aims at presenting the results obtained on the most promising concept of this downselection process. The process started with the evaluation of a large number of potential engine integration concepts, covering a large design space. Subsequently, the configurations are ranked and the most promising are selected for more detailed analyses in

the next steps. In total, three downselections have been performed in the scope of the project, a generic overview of this process is provided in Figure 1.

As a result of the downselection process, the Common Inlet Concept was selected as the most promising concept. The Common Inlet features two turbofans fed by a common circular inlet around the fuselage (see *Figure 2*), split in two parts, one half for each engine. The purpose of that kind of inlet is to ingest the whole boundary layer around the fuselage, in order to maximise the performance benefit of such an extreme BLI concept.



Figure 2 - Comparing a conventional engine installation with the NICE Common Inlet concept.

Based on the previous studies done with the first downselection step, it appeared that on the most important uncertainty is the minimum achievable air inlet length to have an acceptable distortion map in front of the fan face. To cope with this important difficulty, it was decided to first realize the detailed aerodynamic design of the air inlet in cruise conditions using advanced CFD methodologies and then integrate the results in the ONERA Overall Design process to evaluate the performance of the concept at aircraft level.

The first section of this paper is devoted to the aerodynamic design of the Common Inlet done for the LSBJ mission (NICE concept), the second section to the description of the OAD process with a focus on the approaches used to evaluate the BLI benefits. The third and last part is dedicated to presentation of the performance of the concept at aircraft level.

2. Aerodynamic Design of the Common Inlet Concept in transonic conditions

2.1 Overview of the Common Inlet design concept

The aerodynamic design detailed in this paper aims at assessing the benefit of an inlet ingesting the whole boundary layer on the fuselage of a business jet configuration. The inlet must therefore be placed on the rear part of the fuselage. On a real fuselage shape, the wake is a mix of the fuselage boundary layer together with the wing and belly fairing wakes (adding the landing gears and doors wakes at take-off and landing), see *Figure 2*. Such a disturbed wake is for sure a challenge for such an innovative concept, and would add high levels of flow distortion into the engine. The purpose of the study is to assess the benefit that could be expected from the concept. Consequently, the Common Inlet is placed behind a simplified axisymmetric fuselage shape, designed for the purpose of the study.

The design assumptions for the Common Inlet are as follow (see *Figure 3*). Assuming a LSBJ mission, the fuselage length is close to a modern long range Business jet, approximately 23 m. The fuselage diameter is about 2.7 m, and the cylindrical cabin length around 10 m long. The inlet is located at the end of the cylindrical part, in order to have enough inlet length to homogenize the flow before the fan plane. This initial configuration adds a lot of wetted area, but that was considered necessary at the beginning of the study.

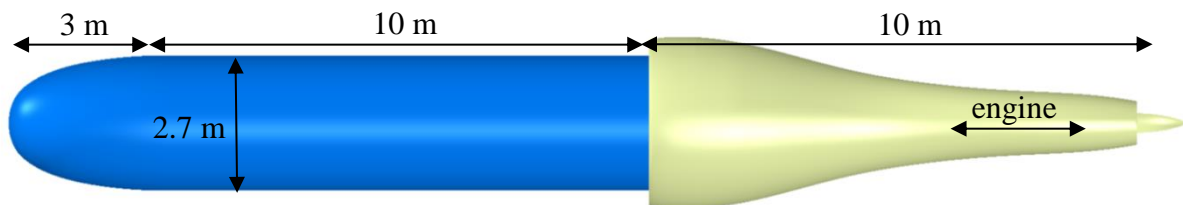


Figure 3 - Side view of the NICE concept.

The engine dimensions are sized with a in-house tool, to be representative of future twin engine business jet with a By-Pass-Ratio (BPR) of 5.5. Assuming a two engine configuration, with a lift-to-drag ratio of 17, ONERA's sizing

tool suggest a fan area of about 1.0 m², a 1.1 m fan diameter (without spinner), and a nozzle area of about 0.6 m² leading to a 0.86 m nozzle diameter. Figures are summarised in Table 1 below.

Table 1 - Main characteristics of the NICE Common Inlet design assumptions.

Cruise conditions	Fuselage length	Fuselage diameter	Engine BPR	Engine cruise FPR	Fan area	Fan diameter	Nozzle area	Nozzle diameter	Fan to nozzle length
Mach=0.8 41000 ft	23 m	2.7 m	5.5	1.7	1.0 m ²	1.1 m	0.6 m ²	0.86 m	2.7 m

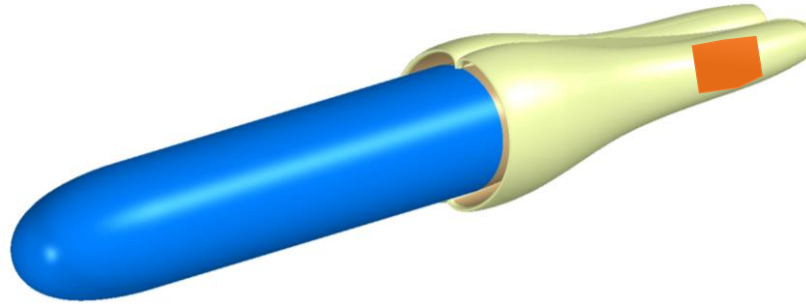


Figure 4 - Overview of the Common Inlet NICE configuration (engine position in orange).

The next section explains how the detailed design of this innovative transonic configuration is managed.

Design process

The design process used in this study relies on previous design experience, such as the NOVA BLI configuration [6], the Nautilus project [12]. The process was modified deeply to account for such a long and distorted inlet shape.

Inlet duct sizing

At first, it is necessary to size the inlet. To achieve that goal, ONERA is using a “stream tube method” design process, which was developed internally to manage the design of BLI inlets. The main assumption is that the stream tube ingested by the intake remains mostly axial in cruise. Consequently, the air intake (in yellow in Figure 5) is placed behind a pipe that has the shape of the inlet front section. The part in contact with the fuselage (in blue on Figure 5) develops a boundary layer, which size can easily be tuned by varying the pipe length.

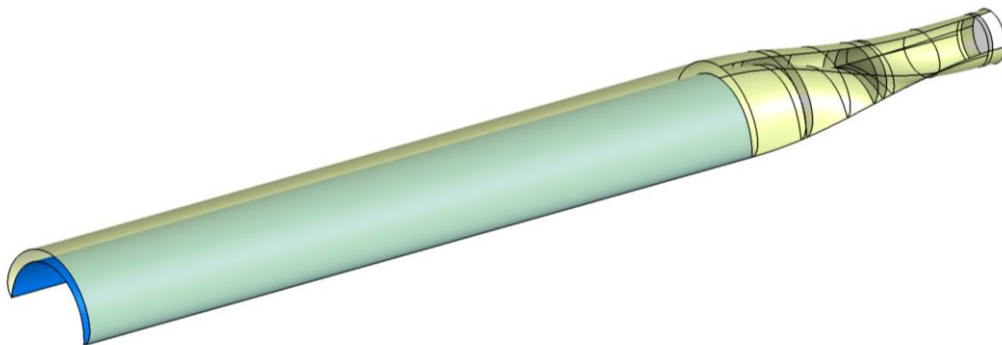


Figure 5 - Intake design using the “Stream tube method” by ONERA.

One lesson learnt from that exercise is that the inlet duct must be a slightly converging duct. Usually, inlet ducts are diverging, in order to slow down the flow before the fan face. For the NICE Common Inlet concept, the flow is already entering at a slow velocity, because most of the flow is composed of a boundary layer, especially in the corners. The inlet maximum height is 240 mm, and swallows a boundary layer that developed on a 13 m long front shape (so the boundary layer height is roughly 130 mm). Figure 6 illustrates that result. With an upstream Mach number of 0.8, the impact of the boundary layer is visible (the “banana shaped” average inlet Mach number is 0.74). Targeting an average fan Mach number of 0.7, the computation reaches $M_{fan}=0.712$. Indeed, boundary layers continue to develop inside that very long intake, which explains why a slightly converging duct is necessary.

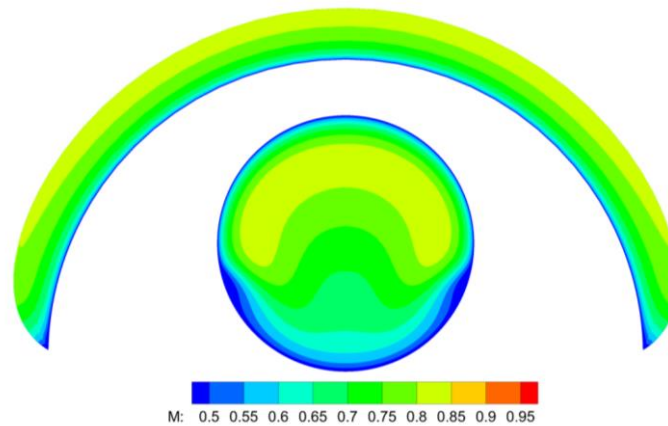


Figure 6 - Front view of a “Stream tube method” result for $M=0.8$.

Outer nacelle design

Starting from the pipe shape obtained with the “stream tube method”, an appropriate profile was added to the lip. Then the outer fairing follows a smooth evolution (yellow fairing in Figure 7). The intake was then symmetrized, and a new fairing was designed to fill the gap between (green fairing in Figure 7). As both nozzles do not touch, an extension fairing was added at the very end (see next part).

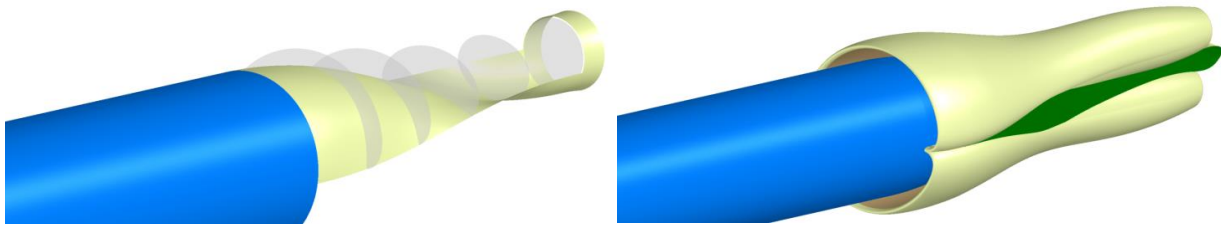


Figure 7 - Designing the outer shape of the inlet up to the nozzle.

Nozzle design

Both nozzle areas are 0.60 m^2 (0.86 m in diameter). For aerodynamic purpose, the choice was made to separate the nozzle. The gap between both nozzles was filled with an extension fairing at the end of the shape (in pink in Figure 8).

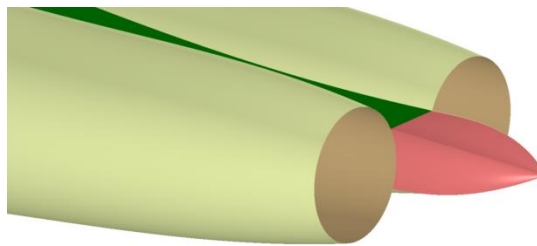


Figure 8 - Nozzle extension fairing.

2.2 CFD evaluation of the Common Inlet

Engine modelling

In a second step, the aerodynamic performance assessment of the configuration was achieved with CFD RANS simulations. For such BLI configuration, the aero-propulsive interactions have to be modelled properly and the classical engine boundary conditions cannot be used (based on mass flow or total pressure). As a consequence, the Body-force approach was used. The principle of the Body-Force is to spread the pressure jump in a volume, therefore, there is no more discontinuity in the volume and the history of the Boundary Layer is preserved from the air inlet up to the nozzle. In practice, source terms are added in the Navier-Stokes equations. These source terms can be determined using different Body-Force models. For this study, a simplified in-house Body-Force model was used, it creates a local volume force in a specified volume.

Mesh strategy

Several meshes were generated with the Pointwise software, with different strategies, such as a quarter configuration, and a half configuration. The final mesh represents the full configuration, including two engines. The resulting unstructured mesh contains $16.5 \cdot 10^6$ elements, mostly tetra and prisms. The wall cell size is $5 \mu\text{m}$, in agreement with the flight Reynolds number of $5.0 \cdot 10^6 \text{ m}^{-1}$. The engine jets are refined (Figure 9). The extent of the mesh refinement in the jets is one fuselage length.

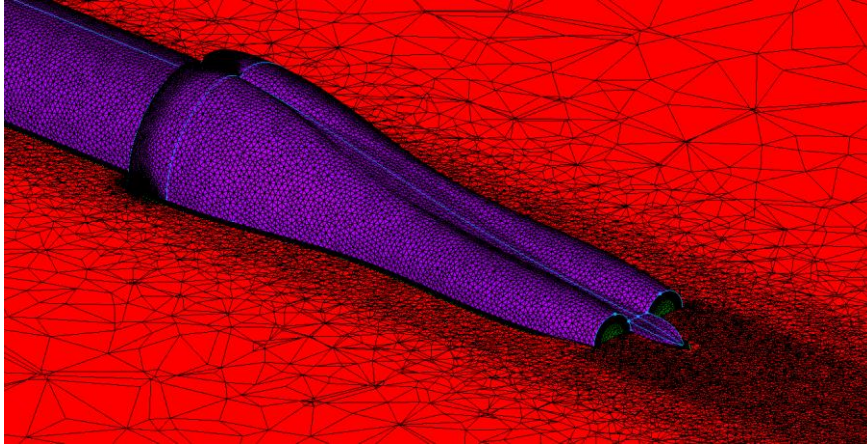


Figure 9 - Mesh density on the engine integration.

Then a pre-processing script adds the body force zone, by tagging some cells. Because the flow will slow down when compressed, it is preferable to place the body force volume in a convergent part of the duct, as illustrated in Figure 10.

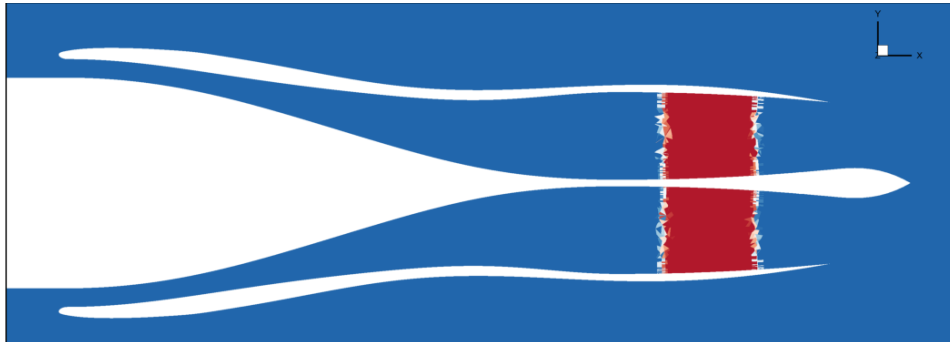


Figure 10 - Body force volume (slice in the horizontal symmetry plane).

The aerodynamic conditions used for the CD computations are summarized in Table 2.

Table 2 - Flight conditions for computations.

Mach number	M	0.80
Altitude	Z	40 000 ft
Static pressure	Ps0	18 752 Pa
Static temperature	Ts0	216.66 K
Total pressure	Pi0	27 246 Pa
Total temperature	Ti0	244.32 K
Metric Reynolds number	Re/m	$5.0 \cdot 10^6 \text{ m}^{-1}$

CFD settings and convergence

The solver is elsA v5.1.02 ([14], ONERA-Safran property). The Jameson scheme with $\kappa_2=0.5$ and $\kappa_4=0.016$ provides a good convergence. The Spalart-Allmaras turbulence model is used. The residuals decrease by at least 3 orders for all simulations.

Body Force values and corresponding engine values

Several computations were performed using growing Body Force values in order to simulate a large range of aircraft thrust/drag equilibrium. The Body Force value is a volume term, which is a force by unit of volume. As it is added to a known volume (the one tagged before the computation, see Figure 10), the corresponding added force is the volume force multiplied by that volume.

Table 3 summarizes the Body Force settings, and the corresponding CFD results. “Local force” is the force obtained by the Body force integrals in the computation. MFR is the absolute Mass Flow Rate for one engine. Epsilon stands for the contraction ratio of the streamtube ingested by the intake. The Mach on fan face is the average Mach number just before the body force. A low value is expected thanks to BLI. The FPR (Fan Pressure Ratio) is obtained by the ratio of total pressure after and before the body force volume. The targeted value without BLI was FPR=1.7. Reaching lower values highlights the benefit of BLI: the fan works at a lower FPR. The Body Force approach figures out the amount of power saving one would obtain with BLI, if a fan were designed to work in those conditions. “Pi on fan face” is an average of the total pressure in front of the body force. It is an indicator of the quantity of ingested boundary layer. For lower MFR, the proportion of slow boundary layer incoming is larger, so the total pressure is lower. The “Pi recovery” is the previous quantity relative to infinite total pressure, and behaves similarly. Without BLI, that figure is expected to be as close to 100% as possible, but with BLI, one seeks to lower it in order to benefit from BLI power saving. The last figure “Intake efficiency” is the total pressure ratio between the beginning of the inlet (leading edge) and the body force. It quantifies the quality of the diverging tube that grows from a “banana” shape to a round circle. That tube being long, boundary layers develop all along. An average intake efficiency of 98.5% is considered satisfactory for such a complex intake geometry. Note that in Table 3, the BF value of 45 000 N/m³ would correspond to the aircraft equilibrium in cruise conditions (i.e. drag = thrust) considering all aircraft components (fuselage, wings, tails, pylon, engines...) and not only the propulsive fuselage.

Table 3 - Summary of the Body Force values and corresponding results. Values italic are specifications, others are extracted from CFD.

<i>BF value (N/m³)</i>	<i>BF volume (daN)</i>	Local force (daN)	MFR (kg/s)	Epsilon A_{∞}/A_{inlet}	Mach on Fan face	FPR	Pi (Pa) on Fan face	Pi recover $P_{i_{fan}}/P_{i_0}$	Intake efficiency
<i>5000</i>	<i>-1077</i>	-1075.4	30.56	0.40	0.341	1.06	24577	86.0%	99.1%
<i>10000</i>	<i>-2154</i>	-2151.5	34.24	0.40	0.341	1.11	24744	86.6%	99.0%
<i>15000</i>	<i>-3232</i>	-3227.3	37.52	0.45	0.341	1.17	24881	87.0%	98.9%
<i>20000</i>	<i>-4309</i>	-4302.3	40.50	0.49	0.377	1.23	24997	87.5%	98.7%
<i>25000</i>	<i>-5386</i>	-5375.7	43.26	0.53	0.411	1.29	25104	87.8%	98.6%
<i>30000</i>	<i>-6463</i>	-6447.1	45.85	0.57	0.445	1.35	25203	88.2%	98.5%
<i>35000</i>	<i>-7540</i>	-7514.9	48.31	0.60	0.478	1.41	25299	88.5%	98.3%
<i>40000</i>	<i>-8618</i>	-8577.1	50.64	0.64	0.512	1.46	25381	88.8%	98.2%
<i>45000</i>	<i>-9695</i>	-9630.7	52.88	0.67	0.546	1.53	25461	89.1%	98.1%
<i>50000</i>	<i>-10772</i>	-10671.2	55.07	0.70	0.582	1.59	25539	89.3%	98.0%

Results

Figure 11 illustrates the total pressure recovery inside the air intake, for FPR=1.53 (BF=45 000 N/m³). In the front part, which has a “banana” shape, the stratification of total pressure demonstrates that the intake swallows all the boundary layer coming from the front part of the fuselage. The total pressure loss in the intake plane is 89.5%. While slowing down in the convergent, the main pressure loss concentrates in the bottom part of the engine (approx. 88% of pressure loss), whereas the top part gets more (approx. 93% of pressure loss). The average total pressure loss in the fan plane is 88.2%. The inlet itself converts 89.5% into 88.2%, which makes an intake total pressure recovery of 98.5%. Figures for all MFRs are in Table 3.

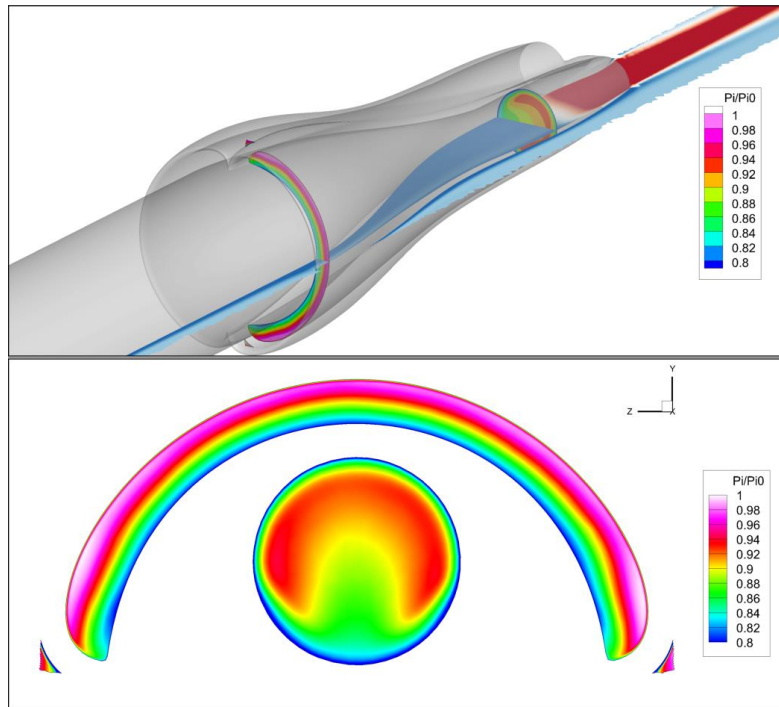


Figure 11 - Intake pressure recovery for $FPR=1.53$ ($BF=45\ 000\ N/m^3$).

One must notice here that the primary core of a jet engine would be fed with lower total pressure than a non-BLI engine. Therefore the power saving on the fan power requirement would be balanced with the power loss on the primary core. An engine deck or model would be necessary to quantify more precisely that effect but it was out of the scope of this study. Figure 12 show the Mach number and total pressure contours in the horizontal plane ($Z=0$) close to equilibrium (i.e. thrust = drag). A proper flow behaviour is observed in these aerodynamic conditions which demonstrates that this design is in line with the initial expectations and can be used for deeper analysis and aerodynamic performance assessment.

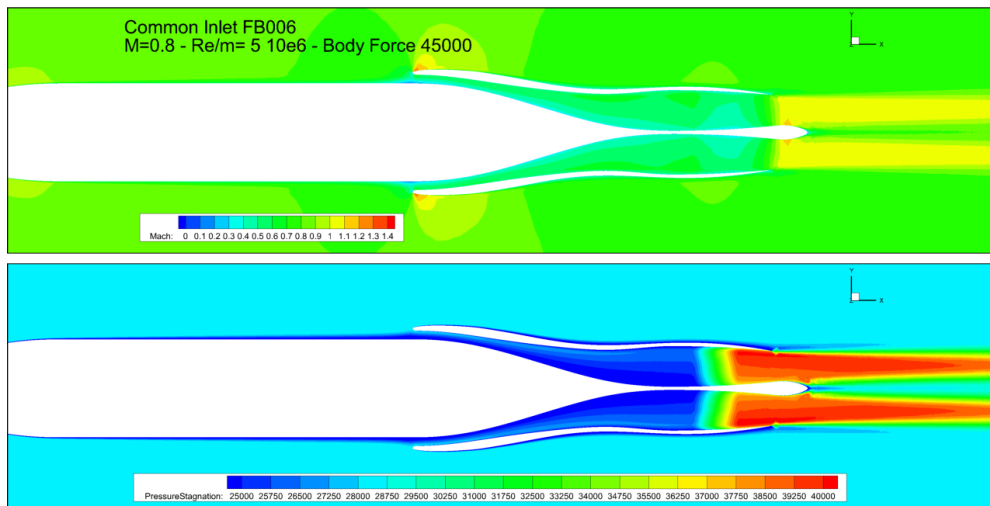


Figure 12 - Horizontal plane for $BF=45\ 000\ N/m^3$ (aircraft equilibrium) - $FPR=1.53$ - $Epsilon=0.67$.

Exergy analysis

For BLI configurations classical thrust/drag bookkeeping cannot be applied. Indeed a part of the drag is swallowed and used for propulsion ([15], [16]) which makes this decomposition irrelevant. More global approaches need to be used to measure the savings with BLI. All previous computations were analysed using the in-house ONERA FFX tool ([17]), which provides an exergy balance for aerodynamic configurations. Exergy is the part of energy that can be transformed into work, which is the mechanical energy. If some exergy remains downstream of the aircraft, it means that this part of the provided energy could have been used in a better way, it has been wasted. The purpose of FFX is to quantify the wasted exergy, which allows quantifying the BLI savins. Exergy can come from velocity

(excess or deficit) and from aerothermics. For BLI configuration, the main driver is the reduction of the exhaust jet velocity, so the analysis presented in this paper focuses on the mechanical exergy coming from velocity terms. Usually, the thermic part is one order of magnitude below the mechanical one for those configurations.

The main term in the exergy balance for BLI is E_u , the mechanical axial exergy, which formula is:

$$\dot{E}_u = \int_{S_O} \rho u^2 (\vec{V} \cdot \vec{n}) dS \quad (1)$$

u denotes the excess or deficit of velocity in the wake. For a boundary layer, $u_{wake} < 0$ but $E_u > 0$. For a jet wake, $u_{jet} > 0$ so $E_u > 0$. Thus in a non BLI case, the deficit of velocity created by boundary layers contributes to a positive value of E_u , meaning that part of that velocity deficit could be used and transformed into work. Besides, the excess of velocity of the jet, which compensates the velocity deficit of aircraft drag (including induced drag and wave drag), is also a source of potential work. In a BLI case, the velocity deficit of the boundary layer is re-energized by the engine. Consequently, u_{wake} and u_{jet} are reduced compared to non-BLI cases. In terms of momentum, at thrust/drag equilibrium, assuming that MFR is the Mass Flow Rate through the engine, $U_{ingested}$ is the velocity deficit ingested by a BLI engine (negative), and u_{jet} the excess of velocity in the jet, the following equations can be formed :

$$\begin{aligned} Drag &\approx \int_{S_{wake}} \rho(V_\infty + u_{wake})(\vec{V} \cdot \vec{n}) dS \approx - \int_{S_{jet}} \rho(V_\infty + u_{jet})(\vec{V} \cdot \vec{n}) dS \approx Thrust \\ Drag(no BLI) &= -Thrust(no BLI) \approx MFR \cdot \left((V_\infty + u_{jet}(no BLI)) - V_\infty \right) \\ Drag(BLI) &= -Thrust(BLI) \approx MFR \cdot \left((V_\infty + u_{jet}(BLI)) - (V_\infty + U_{ingested}) \right) \end{aligned} \quad (2)$$

To get the maximum of BLI power saving, the engine must run at the same MFR as detailed in [18] (see Figure 13).

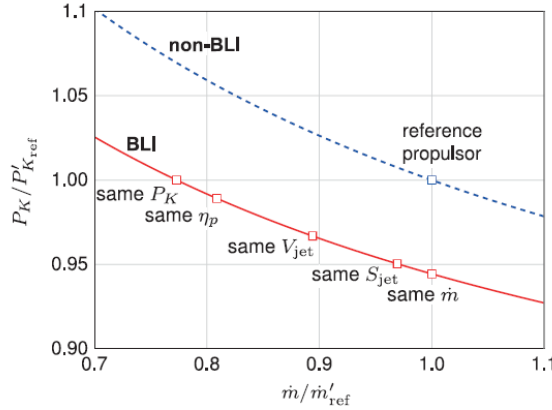


Figure 13 – From [18]: Mechanical flow power vs propulsor mass flow, both normalized by non-BLI reference values, without BLI and with a number of BLI propulsors.

Assuming constant drag for no BLI and BLI configurations (true at first order), and engines of the same MFR, then:

$$\begin{aligned} Drag(no BLI) &= Drag(BLI) \Rightarrow u_{jet}(no BLI) = u_{jet}(BLI) - U_{ingested} \\ So u_{jet}(no BLI) &> u_{jet}(BLI) \end{aligned} \quad (3)$$

As part of the wake is ingested, $u_{wake}(no BLI) < u_{wake}(BLI)$. Assuming $u \ll V_\infty$ and constant values for u_{wake} and u_{jet} in S_{wake} and S_{jet} , and null elsewhere:

$$\begin{aligned} \dot{E}_u(wake) &= \int_{S_{wake}} \rho u_{wake}^2 (\vec{V} \cdot \vec{n}) dS \text{ and } \dot{E}_u(jet) = \int_{S_{jet}} \rho u_{jet}^2 (\vec{V} \cdot \vec{n}) dS \\ so \dot{E}_u(jet no BLI) &> \dot{E}_u(jet BLI) \text{ and } \dot{E}_u(wake no BLI) > \dot{E}_u(wake BLI) \end{aligned} \quad (4)$$

Therefore, the analysis will focus on the mechanical exergy term and more especially on the mechanical axial exergy E_u , thanks to the FFX tool.

FFX analysis on the Common Inlet

From the exergy balance equations, FFX computes a number of physical quantities of interest. Among them:

- W_h is the remaining energy to accelerate or slow down the aircraft. When $W_h=0$, the aircraft is at equilibrium. As the configuration has no wings or tails in the CFD simulation presented in this paper, it is positive for most of the cases.

- E_u is the axial mechanical energy.
- E_{vw} is the transverse mechanical energy (in a plane perpendicular to the upstream velocity). E_{vw} is related to induced drag and to flow vorticity.
- $X_m \sim E_u + E_{vw}$ is the overall mechanical exergy.

All coefficients are expressed in power counts (p.c), with: $Coeff = \frac{Power}{\frac{1}{2}\rho S_{ref} V^3} \cdot 10^4$

Figure 14 summarizes the results obtained for different equilibriums. X_{ff} is the exergy provided by the propulsive part, i.e. the Body Force. E_u and X_m are minimum for $BF=20000 \text{ N/m}^3$. This is an ideal case, for which the ingested flow is re-energised and ejected exactly at the infinite velocity value. However, $W_h < 0$ in that case, meaning the configuration is slowing down. Indeed as already explained a value corresponding to a complete aircraft with wings and tails would stands between $BF=40000 \text{ N/m}^3$ and $BF=45000 \text{ N/m}^3$. In order to assess the power saving due to BLI, that analysis should be compared to a non-BLI configuration. But as the jet velocity reduction is the main driver, an alternative way is to build an theoretical jet wake for a non-BLI configuration.

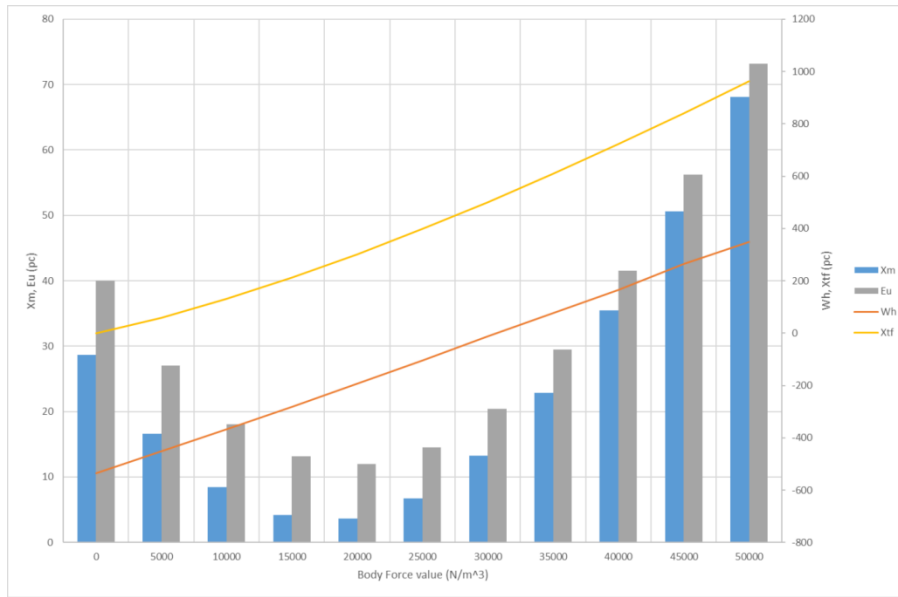


Figure 14 - Far-Field Exergy-based analysis using FFX.

Estimating E_u on a non-BLI configuration

In order to build a fictitious jet for a non-BLI configuration, the jet velocity profile was extracted from the CFD simulation for $BF=45000 \text{ N/m}^3$ (see blue curve in Figure 15). A non-BLI jet wake was then created (red curve on Figure 15), using a Gaussian curve, for which the pseudo-thrust is similar. The integration of both curve using equation (1) enables to give the Power Saving Coefficient (PSC) of the ONERA Common Inlet Concept (assuming that most of the PSC comes from E_u savings):

$$PSC = \frac{Power \text{ no BLI} - Power \text{ BLI}}{Power \text{ no BLI}} \sim \frac{E_u \text{ no BLI} - E_u \text{ BLI}}{E_u \text{ no BLI}} = 13.3\%$$

That order of magnitude is in line with the other configurations already studied at ONERA ([6], [12]) and represents a very important potential benefits of BLI.

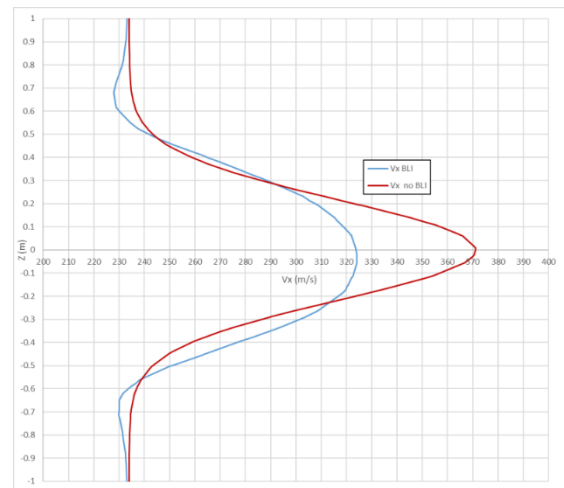


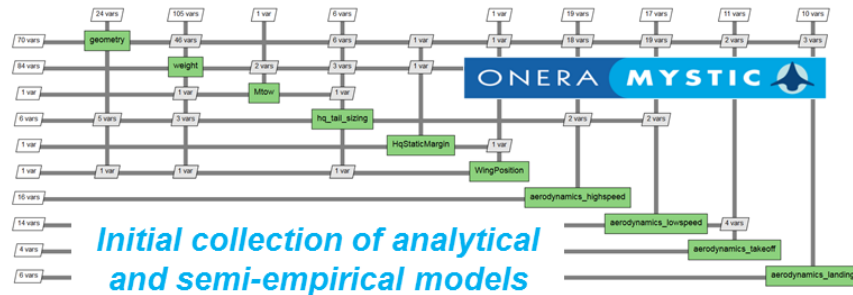
Figure 15 - Jet wake at $X=-1m$ for $BF=45000 \text{ N/m}^3$ - $FPR=1.53$ (blue: BLI from CFD; red: NO BLI reconstructed).

3. Performance of the common inlet concept at aircraft level

3.1 Overall Aircraft Design process

Overview

To assess the performance of the Common Inlet concept for both missions, the MYSTIC OAD process has been used. This tool incorporates physical modules for the classical disciplines of Overall Aircraft Design: Propulsion, Aerodynamics, Mass breakdown and balance, Handling qualities, Trajectory and Performance [19] (Figure 16).



Validated against references
and able to produce T&W derivatives

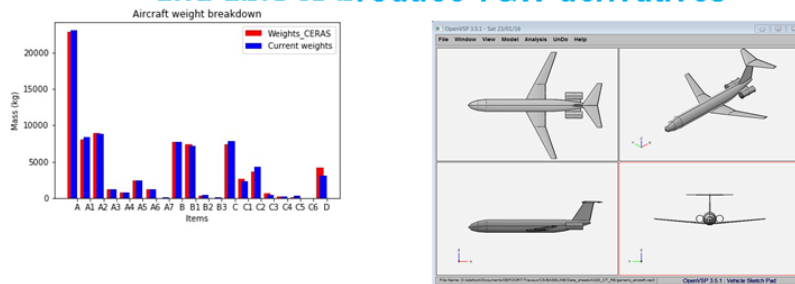


Figure 16 - Inputs and outputs of the MYSTIC tool.

In the process, three sizing loops are implemented, allowing designing an aircraft upon its TLARs with iterations on the disciplinary modules. As the logic of the down-selection process is to progressively increase the level of fidelity of the different modules while decreasing the number of selected configurations, 3 levels of BLI modules have been defined (Figure 17). All these BLI modules are detailed and validated in [20] and are not re-described in this paper.

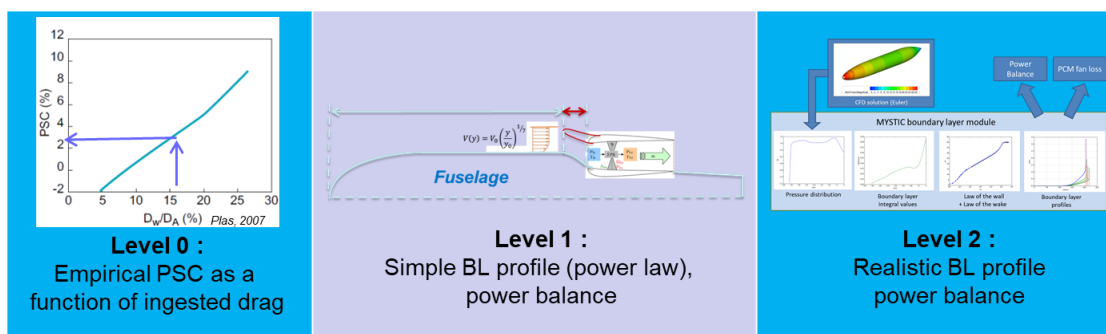


Figure 17 - BLI modules - The three levels of fidelity for BLI modeling in the OAD tool MYSTIC.

Parameterization for BLI architectures at aircraft level

The starting point of all modules is the definition of a geometric parameterization of the BLI arrangement. Two main parameters are necessary:

- The embedding ratio defining which part of the nacelle is buried into the fuselage body (front view), and driving the average flow that will be seen by the engine inlet ;
- The k-ingestion ratio defining the amount of BLI ingested by the engine inlet (k=0 means the nacelle is considered as circular at the same size as the fan, k=1 means that 100% of the fuselage boundary layer is ingested).

For the Common Inlet concept, the value of these two parameters is 1. The nacelle is completely buried into the fuselage and 100% of the fuselage boundary layer is ingested. Based on this simplified geometric parameterization all processes allow to compute the Power Saving Coefficient “PSC” (equation (5)), which is based on the estimation of the reduction of the propulsive power required to sustain the flight at constant speed and altitude.

$$\text{PSC}(\%) = \frac{\text{Power}_{\text{noBLI}} - \text{Power}_{\text{BLI}}}{\text{Power}_{\text{noBLI}}} \quad (5)$$

3.2 Performance assessment at conceptual level

This section presents the final performance of the Common Inlet for both missions obtained using only the L2 module described in [20] in the frame of the OAD MYSTIC process. These performances are compared with those of the reference (non-BLI) aircraft. In this evaluation, different assumptions were made regarding the additional length of the air inlet with the Common Inlet Concept and the location of the engine to be consistent with the detailed aerodynamic design presented in §2. In practice, the maximum air inlet length (“Long Inlet” in the figures above) corresponds to the design presented in §2 and the engines are moved backward by half of this additional air inlet length (meaning implicitly that air inlet is moved forward by half of this additional air inlet length compared to a classical air inlet).

LSBJ mission

Figure 18 to Figure 23 show respectively the differences in terms of MTOW (Maximum Take-Off Weight), OWE (Operational Weight Empty), Fuel Burn, SFC (Specific Fuel Consumption), LoD (Lift over Drag in cruise) and PSC (Power Saving coefficient) between the reference aircraft and the three Common Inlet configurations (respectively with the short, medium and long air inlets) for different engine BPRs (By-Pass Ratio).

The Common inlet configuration enables a fuel burn reduction (Figure 20) between 6 and 14%. These benefits are strongly dependent on the length of the air inlet and tends to be reduced when the BPR increases (by about 1.5% between BPR 4 and 8). The penalties on the SFC are due to distortions in front of the fan face and a reduction of the fan efficiency. These penalties increase with the BPR.

With the long air inlet described in §2, the fuel burn reduction is between 5 and 6% with a PSC of about 11.5% which is consistent with the exergy-based analysis presented above (13%) but without a precise description of the complete aircraft (except the propulsive fuselage).

These results highlight that the potential of the Common Inlet is very high in terms of fuel burn reduction. The first design activities performed in §2 shows the feasibility of the concept but to go further into details, refined design activities would be needed by considering the complete flight envelop and by ensuring that the core of the engine will not (or slightly) be affected by stagnation pressure losses. In such a case, the benefits of the Common Inlet concept would be reduced proportionally to these stagnation pressure losses

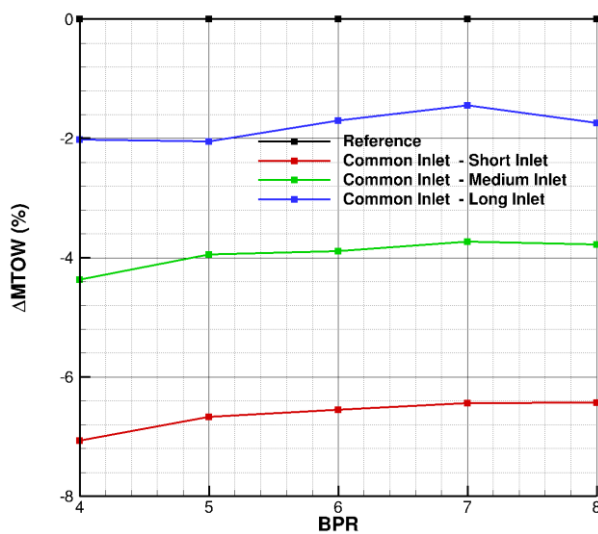


Figure 18 - LSBJ - MTOW variations wrt the reference.

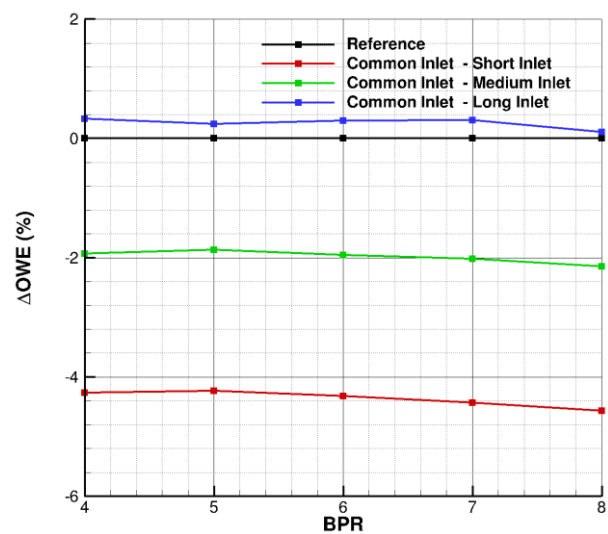


Figure 19 - LSBJ - OWE variations wrt the reference.

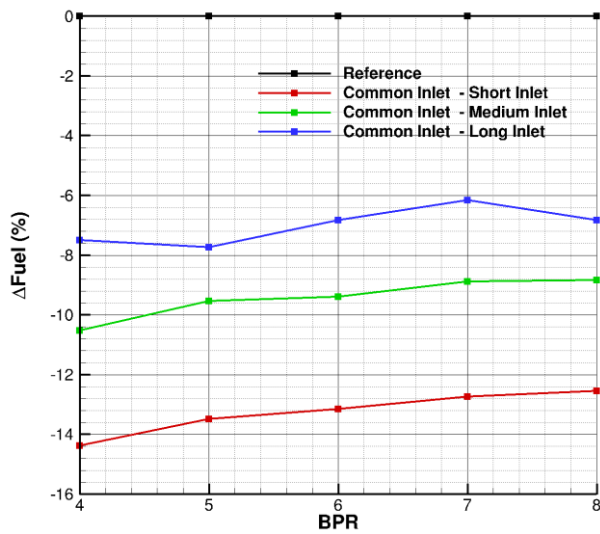


Figure 20 - LSBJ - Fuel Burn variations wrt the reference.

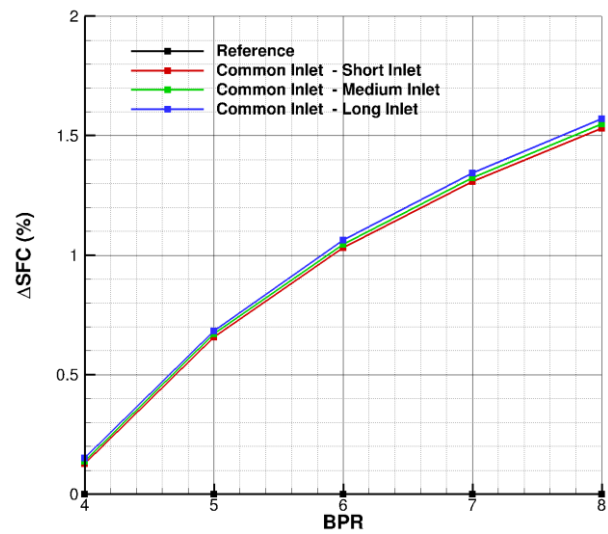


Figure 21 - LSBJ - SFC variations wrt the reference.

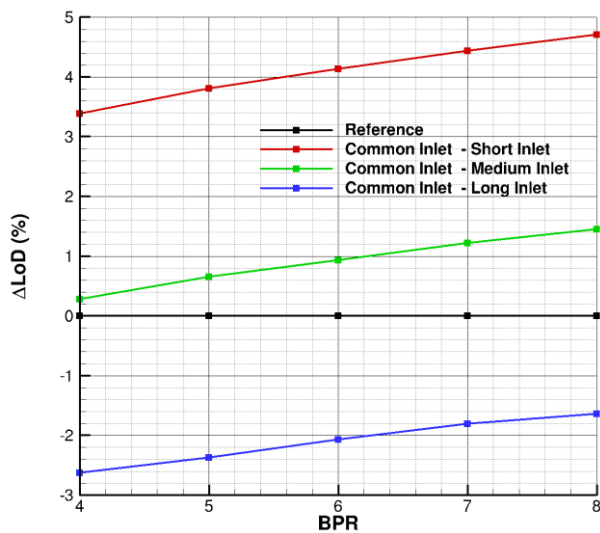


Figure 22 - LSBJ - LoD variations wrt the reference.

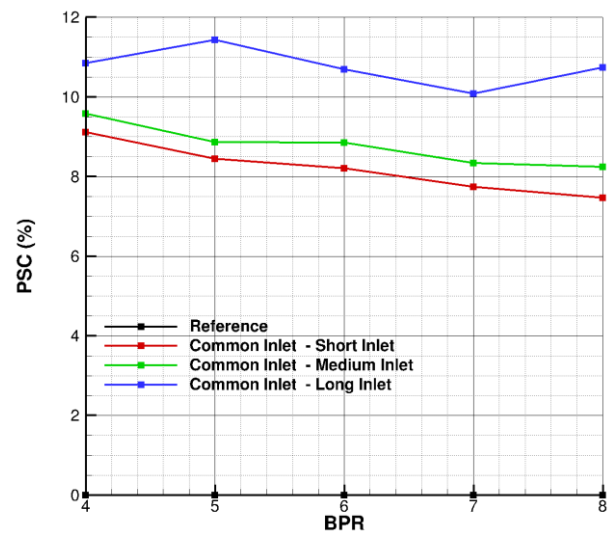


Figure 23 - LSBJ - PSC.

SMR-like mission

As for the business configuration, Figure 24 to Figure 29 show the evolution of the differences between the Common Inlet concepts and the reference aircraft configurations - respectively for the MTOW, OWE, Fuel Burn, SFC, LoD and PSC - with respect to the BPR (from 5, corresponding to the engine of the CeRas reference configuration up to 20, corresponding to advanced 2035 / 2045 turbofan engine technology).

For this mission, two reference aircraft are used:

- the first one corresponds to classical SMR-like aircraft with UnderWing mounted engines and a conventional tail (referred hereafter as UW reference) ;
- The second one to a rear-fuselage mounted engines aircraft with a T-tail (referred hereafter as RE reference).

Moving the engine to the back induces a penalty of about 3% in terms of Fuel Burn for all BPR values as expected. This penalty is due to an increase of the HTP / VTP areas and masses implying a reduction of the LoD and an increase of the OWE. As the 'real' reference aircraft is the underwing mounted engine one, the benefits of the Common Inlet concept are less important for the SMR mission than for the business one.

Indeed, Figure 26 shows that only with the short and medium inlet length options a fuel burn reduction can be obtained. Furthermore, these benefits decrease with the BPR values for two main reasons:

- the PSC decreases with the BPR as the jet velocities downstream of the engine, thus the potential of BLI is progressively reduced with the BPR increase (see Figure 29) ;

- The diameter of the fan increases with the BPR, meaning that the wetted area of the nacelle (including the air inlet) also increases which has a negative impact of the LoD (see Figure 28) and thus on the fuel consumption (see Figure 26).

Compared to the UW reference aircraft, the maximum fuel burn reduction reaches 9% for BPR=5 (corresponding to 2000's reference) but only 6.5% with BPR = 15 (2025's reference) with the short inlet. The BLI benefits are more important if the RE reference aircraft is considered as the reference, the fuel burn benefits are about 12.5% for BPR=5 and 10% for BPR=15 with the short inlet option. With the medium inlet the benefits are reduced respectively to 4 and 2% for BPR equal to 5 and 15.

The results shows the potential of the Common Inlet concept is less important for the SMR mission that for the business jet one as the location of the engine represents an important penalty and as the high BPR values of future engine limits the benefits of BLI.

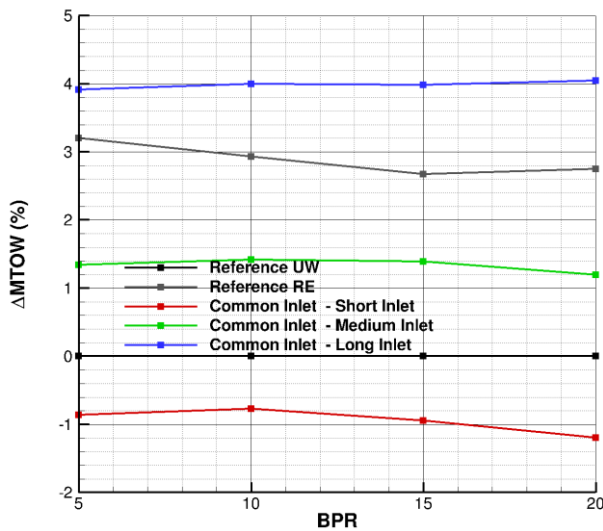


Figure 24 - SMR - MTOW variations wrt the reference.

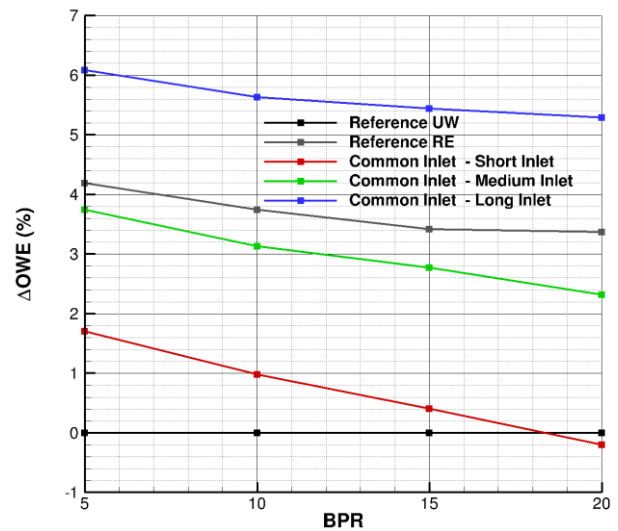


Figure 25 - SMR - OWE variations wrt the reference.

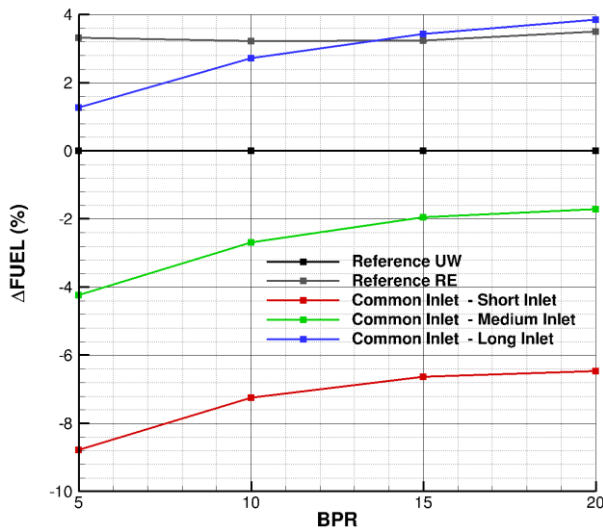


Figure 26 - SMR - Fuel Burn variations wrt the reference.

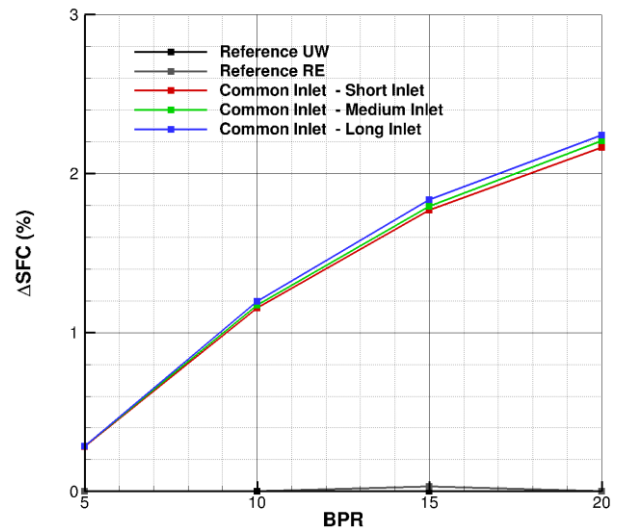


Figure 27 - SMR - SFC variations wrt the reference.

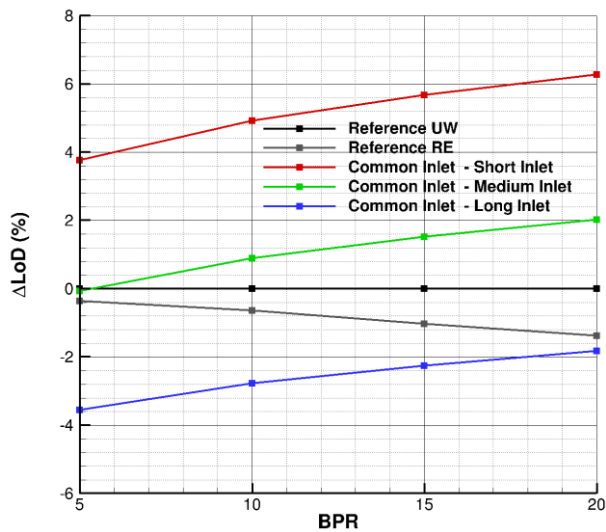


Figure 28 - SMR - LoD variations wrt the reference.

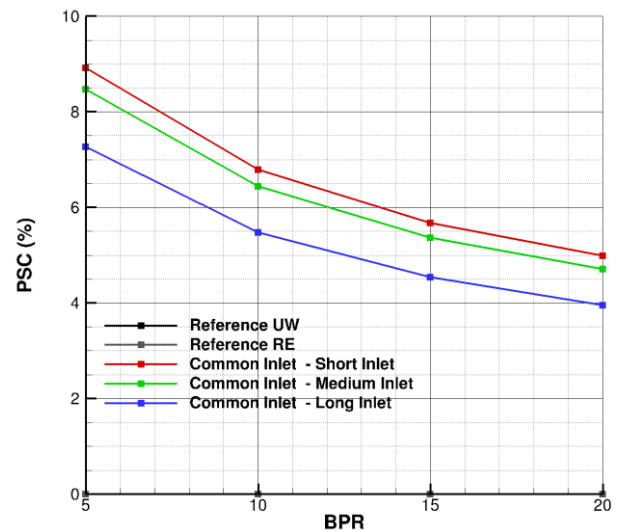


Figure 29 - SMR - PSC.

4. Conclusions

In the frame of the Clean Sky 2 programme, ONERA in collaboration with DLR, Airbus and Dassault Aviation has studied different BLI concepts for two missions (business jet and SMR-like). After a down-selection process, the level of fidelity of the tools used to evaluate the performance of the different concepts was increased. Meanwhile, the number of selected concepts was reduced, and the Common Inlet concept was selected as the most promising one for both missions.

This paper focuses on the detailed aerodynamic design of the propulsive fuselage including the air inlet of the configuration, and on performance assessment at aircraft level using advanced OAD models to capture the physical phenomena driving the performance of BLI concept. First, a detailed description of the aerodynamic design activities is provided together with an exergy-based analysis. The results highlight that the achievable PSC coefficient of such a configuration is relatively high (about 13%) in cruise conditions and similar to the initial expectations. Nevertheless, these design activities have also shown that the length of the air inlet has to be relatively long to obtain a reasonable distortion map in front of the fan face and that potential stagnation pressure losses upstream of the core engine could further reduce the potential of the Common Inlet concept.

The OAD activities performed for both missions have confirmed these trends. The ability to reduce the air inlet length without degrading too much the engine performance remains the main challenge as the impact on the overall aircraft performance are significant. Nonetheless, for the business jet mission, the benefits of the Common Inlet concept remain important as rather low BPR values have to be considered, a maximum of about 13% can be achieved with a very short inlet and 8% with a long inlet for classical BPR values. In this evaluation, the impact of the distortions on the fan efficiency has been considered but not the potential stagnation pressure losses upstream of the core engine. For the SMR mission, the potential of the concept is less important as the rear fuselage engine position implies an important penalty as well as the high BPR values which further reduce the pure potential of BLI. The maximum achievable gains for BPR=15 are about 6.5% with a very short inlet.

To consolidate the benefits, additional design activities are required by considering the full flight envelope and not only cruise conditions, as well as the potential penalties due to the stagnation pressure losses upstream of the core engine. In terms of structural design, important efforts should also be done to have a first structural concept available and consolidate the initial assumptions (no specific mass penalties due to the Common Inlet concept).

5. Acknowledgement

The project leading to this application has received funding from the Clean Sky 2 Joint Undertaking under the European Union's Horizon 2020 research and innovation program under grant agreement N°CS2-AIR-GAM-2022-2023. The authors would like to thank the project partners from DLR (M. Iwanizki, D. Silberhorn, T. Zill, from Dassault Aviation (Jean Le Gall, Michel Ravachol) and from AIRBUS (Lars Joergensen, M. Werner) for their interest in this topic and their guidance.

5. References

- [1] Smith L. H. Jr., "Wake Ingestion Propulsion Benefit", *Journal of Propulsion and Power*, Vol. 9, No. 1, 1993, pp. 74–82.
- [2] J. I. Hileman, Z. S. Spakovszky, M. Drela, "Airframe Design for "Silent Aircraft" ", AIAA 2007-453, 2007.
- [3] David J. Arend, Gregory Tillman, Walter F. O'Brien, "Generation After Next Propulsor Research: Robust Design for Embedded Engine Systems", AIAA 2012-4041, 2012.
- [4] Uranga A., et al. Preliminary Experimental Assessment of the Boundary Layer Ingestion Benefit for the D8 Aircraft, 52nd Aerospace Sciences Meeting, January 13-17, 2014, National Harbor, Maryland.
- [5] Plas, A., Crichton, D., Sargeant, M., Hynes, T., Greitzer, E., Hall, C. and Madani, V. 2007. Performance of a Boundary Layer Ingesting (BLI) Propulsion System. 45th AIAA Aerospace Sciences Meeting and Exhibit (Reno, Nevada, Jan. 2007). ISBN 9781624100123. DOI 10.2514/6.2007-450.
- [6] Atinault O., Carrier G., Grenon R., Verbeke C. and Viscat P., "Numerical and Experimental Aerodynamic Investigations of Boundary Layer Ingestion for Improving Propulsion Efficiency of Future Air Transport", 31st AIAA Applied Aerodynamics Conference, June 24-27, 2013, San Diego, CA.
- [7] Isikveren, A.T., Seitz, A., Bijewitz, J., Mirzoyan, A., Isyanov, A., Grenon, R., Atinault, O., Godard, J.-L. and Stückl, S. 2015. Distributed propulsion and ultra-high by-pass rotor study at aircraft level. *The Aeronautical Journal*. 119, 1221 (Nov. 2015), 1327–1376. ISSN 0001-9240, 2059-6464. DOI 10.1017/S0001924000011295.
- [8] Blumenthal, B., Elmiligui, A.A., Geiselhart, K., Campbell, R.L., Maughmer, M.D. and Schmitz, S. 2016. Computational Investigation of a Boundary Layer Ingestion Propulsion System for the Common Research Model. 46th AIAA Fluid Dynamics Conference (Washington, D.C., Jun. 2016). ISBN 9781624104367. DOI 10.2514/6.2016-3812.
- [9] Welstead, J. and Felder, J.L. 2016. Conceptual Design of a Single-Aisle Turboelectric Commercial Transport with Fuselage Boundary Layer Ingestion. 54th AIAA Aerospace Sciences Meeting (San Diego, California, Jan. 2016). ISBN 9781624103933. DOI 10.2514/6.2016-1027.
- [10] M. Méheut and al. "Conceptual Design Studies of Boundary Layer Engine Integration Concepts", Aerospace Europe Conference 2020, 25-28 February 2020, Bordeaux, France.
- [11] Wiart, L., Atinault, O., Boniface, J.-C. and Barrier, R. 2016. Aeropropulsive performance analysis of the NOVA configurations. 30th Congress of the International Council of the Aeronautical Sciences (Daejeon, South Korea, Sep. 2016).
- [12] Wiart, L. and Negulescu, C. 2018. Exploration of the Airbus "NAUTILIUS" Engine Integration Concept. 31st Congress of the International Council for Aeronautical Sciences (Belo Horizonte, Brazil, Sep. 2018).
- [13] Risse, K., Schäfer, K., Schültke, F., and Stumpf, E., "Central Reference Aircraft data System (CeRAS) for research community.", In: CEAS Aeronautical Journal 7(1), pp. 121–133, 2016. DOI: 10.1007/s13272-015-0177-9.
- [14] Cambier, L., Heib, S., and Plot, S., "The ONERA elsA CFD Software: Input from Research and Feedback from Industry," *Mechanics and Industry*, Vol. 15(3), pp. 159-174, 2013.
- [15] Drela, M., "Power Balance in Aerodynamic Flows", *AIAA Journal*, Vol. 47, No. 7 (2009), pp. 1761-1771.
- [16] Arntz, A., "Civil Aircraft Aero-thermo-propulsive Performance Assessment by an Exergy Analysis of High-fidelity CFD-RANS Flow Solutions", PhD Thesis, Lille 1 University, 2014.
- [17] Ilias Petropoulos, Christelle Wervaecke, Didier Bailly, Thibaut Derweduwen. "Numerical investigations of the exergy balance method for aerodynamic performance evaluation". AIAA AVIATION 2019, June 2019, DALLAS, United States. (10.2514/6.2019-2926).
- [18] Hall, D. K., Huang, A. C., Uranga, A., Greitzer, E. M., Drela, M., & Sato, S. (2017). "Boundary layer ingestion propulsion benefit for transport aircraft". *Journal of Propulsion and Power*, 33(5), 1118-1129. <https://doi.org/10.2514/1.B36321>.
- [19] S. Defoort, M. Méheut, B. Paluch, R. Liaboeuf, R. Murray, D.-C. Mincu, J.M. David, "Conceptual design of disruptive aircraft configurations based on High-Fidelity OAD process", AIAA Aviation Forum, Atlanta, 2018.
- [20] O. Atinault, M. Méheut and S. Defoort, "A Mixed Fidelity Conceptual Design Process for Boundary Layer Ingestion Concepts", ECCOMAS Congress 2022, June 2022, Oslo, Norway.